



The Society shall not be responsible for statements or opinions advanced in papers or discussion at meetings of the Society or of its Divisions or Sections, or printed in its publications. Discussion is printed only if the paper is published in an ASME Journal. Authorization to photocopy material for internal or personal use under circumstance not falling within the fair use provisions of the Copyright Act is granted by ASME to libraries and other users registered with the Copyright Clearance Center (CCC) Transactional Reporting Service provided that the base fee of \$0.30 per page is paid directly to the CCC, 27 Congress Street, Salem MA 01970. Requests for special permission or bulk reproduction should be addressed to the ASME Technical Publishing Department.

Copyright © 1997 by ASME

All Rights Reserved

Printed in U.S.A.

**PREDICTION OF THE BECALMED REGION FOR  
LP TURBINE PROFILE DESIGN**



**Volker Schulte**  
BMW Rolls-Royce GmbH  
15827 Dahlewitz, Germany

**Howard P. Hodson**  
Whittle Laboratory  
Cambridge University Engineering Department  
Madingley Road  
Cambridge CB3 0DY, UK

**ABSTRACT**

Recent attention has focused on the so called 'becalmed region' that is observed inside the boundary layers of turbomachinery blading and is associated with the process of wake-induced transition. Significant reductions of profile loss have been shown for high lift LP turbine blades at low Reynolds-numbers due the effects of the becalmed region on the diffusing flow at the rear of the suction surface.

In this paper the nature and the significance of the becalmed region are examined using experimental observations and computational studies. It is shown that the becalmed region may be modelled using the unsteady laminar boundary layer equations. Therefore, it is predictable independently of the transition or turbulence models employed. The effect of the becalmed region on the transition process is modelled using a spot-based intermittency transition model. An unsteady differential boundary layer code was used to numerically simulate a deterministic experiment involving an isolated turbulent spot.

The predictability of the becalmed region means that the rate of entropy production can be calculated in that region. It is found to be of the order of that in a laminar boundary layer. It is for this reason and because the becalmed region may be encroached upon by pursuing turbulent flows that for attached boundary layers, wake-induced transition cannot significantly reduce the profile loss. However, the becalmed region is less prone to separation than a conventional laminar boundary layer. Therefore, the becalmed region may be exploited in order to prevent boundary layer separation and the increase in loss that this entails. It is shown that it should now be possible to design efficient high lift LP turbine blades.

**NOMENCLATURE**

- A area
- $Re_2$  Reynolds-number at exit based on chord

- $Re_{th}$  Momentum thickness Reynolds-number
- S Absolute entropy
- s stream-wise co-ordinate
- $\%s$  fraction surface length
- T Temperature
- t time
- $U_\infty$  free-stream velocity
- u stream-wise velocity component
- $Y_p$  suction surface boundary loss coefficient
- y surface normal co-ordinate
- $\mu$  molecular viscosity
- $\nu$  kinematic viscosity
- $\rho$  density

**Subscripts**

- eff effective
- lam laminar
- tr transition
- turb,t turbulent
- time mean

**INTRODUCTION**

In a modern civil engine, the LP turbine operates at subsonic Mach-numbers and usually consists of several stages so that the associated weight and cost is large. Furthermore, their efficiency strongly influences the specific fuel consumption. There is a significant incentive for improving the aerodynamic design of this component.

Due to the large aspect ratios in LP turbines, the profile loss is by far the largest portion of the total. The magnitude of profile loss depends upon the development of the airfoil boundary layers. Changes in the process of boundary layer transition and separation can alter the profile loss significantly for the same profile shape at different

Presented at the International Gas Turbine & Aeroengine Congress & Exhibition  
Orlando, Florida — June 2–June 5, 1997

This paper has been accepted for publication in the Transactions of the ASME  
Discussion of it will be accepted at ASME Headquarters until September 30, 1997

Downloaded from http://asmedigitalcollection.asme.org/GT/proceedings-pdf/GT/1997/78882V001T03A060/2408513A001103A060-97-gt-398.pdf by guest on 16 August 2022

operating conditions. Consequently the search for further improvements in loading and efficiency of LP turbines should consider the details of the processes of boundary layer transition and separation.

The performance targets of modern LP turbine blading do not only concern efficiency, but also weight and manufacturing costs. It is desirable to use less blades per blade row so that an individual blade has to carry a greater aerodynamic load. Increased lift coefficients can only be realised if the pressure distribution has regions of significant diffusion on the suction surface. This inevitably increases the risk of laminar separation. In order to avoid significant deterioration in efficiency due to large separation bubbles (or even non-reattached separation), the concept of controlled boundary layer design has been introduced in industry (Hourmouziadis, 1989).

To date, LP turbines have been designed using steady flow assumptions. However, it is now well known that the boundary layers on turbomachinery blades are by no means steady (e.g., Hodson et al., 1994, Halstead et al., 1995, Banieghbal et al., 1995). The turbulence associated with the wakes shed by upstream blade rows is responsible for much of the unsteady nature of the transition process. It is now known that the profile loss in the turbine can be either higher (Hodson, 1984) or lower (Schulte and Hodson, 1996) than in a steady state cascade test. Schulte and Hodson (1996) show that at typical LPT Reynolds-numbers ( $Re=0.8-3 \times 10^5$ ) the wake-passing induces periodic transition. The wakes do not create turbulent flow but patches of bypass transition within the boundary layer where turbulent spots appear, grow and coalesce to form turbulent patches. So-called 'becalmed regions' trail the turbulent spots/patches as they move over the blade surface.

The becalmed region is a laminar-like region with a very full velocity profile that follows after the turbulent flow. Initially it is associated with a high wall shear stress (similar to that of the turbulent flow) that then relaxes back to a laminar value (Seifert, 1994, Cumpsty et al. 1995, Halstead et al. 1995, Schulte, 1995, Gostelow et al. 1996). Whereas the transitional/turbulent patches tend to increase losses, the becalmed regions tend to reduce losses compared to the undisturbed boundary layer as it is present in steady state cascade tests. It is the trade off between these two effects which is important for the loss. The trade off depends mainly upon the Reynolds-number, the wake-passing frequency and the wake strength, and the pressure distribution of the blades.

Schulte and Hodson (1996) showed that for high lift blading at low Reynolds-numbers, when a large suction side separation bubble exists, the loss in the turbine may be significantly lower than in the steady flow cascade test. Consequently the beneficial effect of the becalmed region outweighs the detrimental effect of the transitional patches.

Having recognised the potential to design efficient high lift blading even at very low Reynolds-numbers by exploiting the effect of the becalmed regions it is now necessary to set up design criteria and develop predictive tools that account for the mechanisms of unsteady transition including the becalmed regions.

The present paper explores the significance of the becalmed region and presents a transition model allowing for the effects of the becalmed regions. The model is validated and consequences for the design of LP turbines are discussed.

## MODELLING OF THE BECALMED REGION

Becalmed regions behind isolated turbulent spots were first found by Schubauer and Klebanoff (1955). They provided an explanation for the existence of the becalmed regions which was linked to the existence of Tollmien-Schlichting waves. This was recently discredited by Schulte (1995) and Gostelow et al. (1996). The effect of the becalmed regions on the unsteady wake-induced transition process was first illustrated by Pfeil et al. (1982).

The lack of susceptibility to small disturbances within a becalmed region means that turbulent spots can probably not form inside a becalmed region and boundary layer separation is probably prevented or delayed within them. On the other hand, the becalmed region will be terminated (made turbulent) by other turbulent spots that move into it from behind. For transition in steady external flow turbulent spots only form in the vicinity of a single stream-wise position according to the hypothesis of Narasimha (1957). Hence, the becalmed region does not have a noticeable effect, since spots do not form anyway within their domain of influence. This process is illustrated in the simplified distance-time ( $s-t$ ) diagram of fig. 1.

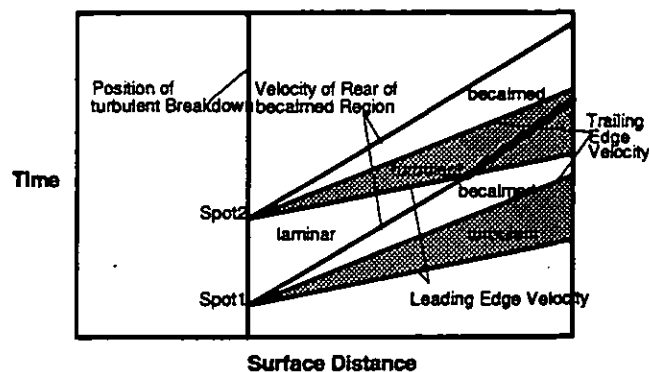


Figure 1: Schematic of steady flow transition situation showing two individual turbulent spots

Only the unsteady scenario gives rise to a visible effect of the becalmed regions. Figure 2 illustrates this using another simplified distance-time diagram. For some reason (e.g. wake passing) spot 1 has been formed at position  $s_1$  upstream of the position of turbulent breakdown ( $s_2$ ) for the otherwise undisturbed flow. Along this line spots form at a rate which is given by  $1/\Delta t$ . This gives rise to the natural transition process being completed at the position  $s_3$ . The becalmed region of spot 1 inhibits spot production at position  $s_2$  for the time  $\Delta t_{calm}$ . Therefore the disturbed (unsteady) transition process is only completed at position  $s_4$ .

Finally it has to be recognised that the susceptibility of the becalmed region to various disturbances will probably vary with streamwise distance. It might therefore happen that the becalmed region has weakened sufficiently to allow spots to form along, say a line AB in fig. 2. There is evidence that this happens, especially in compressors, where wake-induced transitional/turbulent patches seem to form further upstream and travel a longer distance until they reach the position of natural transition (e.g. Halstead et al., 1995).

In summary, the probability for a becalmed region is able to inhibit spot production and separation seems to be very high as is the

probability that it is terminated (made turbulent) by neighbouring turbulent spots that move into it.

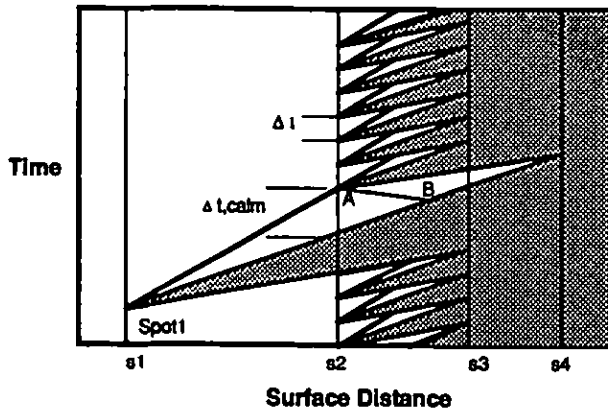


Figure 2: Schematic of (unsteady) transition situation with one turbulent spot being formed upstream of others

Following the above arguments, a probability based (spot-based) intermittency model that includes the effects of becalmed regions is derived in the appendix. The intermittency distribution obtained as described in the appendix only models the becalmed region in terms of its effect on the transition process by way of its effect on the spot production rate. No specific model to account for the ability of the becalmed region to suppress separation is included. This is unnecessary because, as the next section will show, the becalmed region is modelled by the unsteady laminar boundary layer equations.

## NUMERICAL SIMULATION OF THE BECALMED REGION

### Unsteady Differential Boundary Layer Code and Implementation of the Intermittency Model

The following calculations are performed with an adaptation of the well proven unsteady differential boundary layer code by Cebeci and Carr (1978). A similar version of the code has previously been used by Addison and Hodson (1992). The code employs an eddy-viscosity turbulence model. The current version is only able to calculate attached boundary layers.

The code has been adapted to enable it to calculate unsteady transitional boundary layers (including becalmed regions). This is done by calculating an unsteady intermittency distribution prior to the calculation with the boundary layer code. The calculated intermittency distribution is then prescribed for the boundary layer calculation. The intermittency distribution is used to weigh the eddy viscosity according to

$$v_{eff}(s, y, t) = v_{lam} + \tilde{\gamma}(s, t)v_{urb}(s, y, t), \quad (1)$$

where  $v_{urb}(s, y, t)$  is determined using the instantaneous velocity profiles.

The intermittency distribution used in equation (1) is determined in a separate routine and combines correlations for transition onset and the initial spot production rate with the intermittency model outlined in the appendix. Details of the correlations used for transition

onset, the spot production rate and the shape of the dependence volume can be found in Addison and Hodson (1992) and Schulte (1995). These are omitted here, because they are not needed for the simulation of the deterministic experiment described in the following section.

### Numerical Simulation of a Deterministic Experiment

The experiment conducted by Seifert (1994) was simulated numerically in order to validate the model of the becalmed regions that has been introduced above. Seifert investigated an individual artificially generated turbulent spot that moves through an initially laminar and then transitional boundary layer. His test case constitutes of a flat plate with an imposed adverse pressure gradient simulating the rear part of the suction surface of a turbine blade. The velocity distribution as measured and predicted by Seifert is shown in fig. 3. In undisturbed flow the transition onset is located at approximately 70% $s$ . Downstream of this the boundary layer is transitional and reaches a fully turbulent state by the trailing edge. Time-resolved measurements of the velocity profiles at various streamwise stations utilising a single hot-wire were presented. The velocity profiles are ensemble averaged.

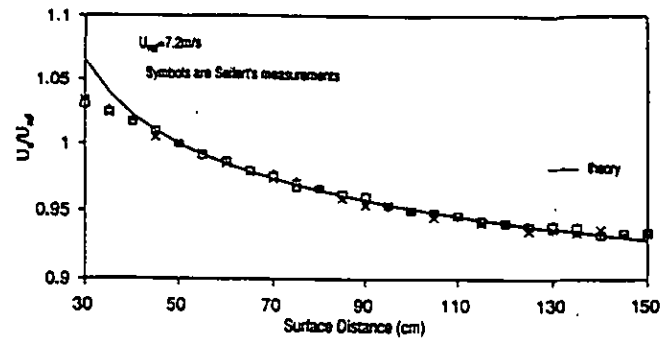


Figure 3: Velocity distribution of Seifert's flat plate test case (Seifert, 1994)

Using the velocity distribution of Seifert's plate and specifying the measured location of transition onset and a suitable spot production rate in the intermittency model (see appendix), the undisturbed boundary layer development of the test case could be matched using the current boundary layer prediction system.

In the spot-disturbed case, an individual turbulent spot was triggered at 20% $s$ . This was simulated using the intermittency routine by specifying that the spots are created at 20% $s$ . This resulted in an intermittency distribution as shown in fig. 4. Inside the spot affected region the intermittency is unity. The becalmed region suppresses spot-production completely for some time at 70% $s$ . Otherwise the intermittency distribution is as in the undisturbed case downstream of 70% $s$ .

In this simulation of an individual turbulent spot, the spot is assumed to be identical to the a completely turbulent span-wise strip. Hence, in order to implement the effect of the individual turbulent spot on the intermittency distribution, an integration of the volumes of dependence, as outlined in the model in the appendix, is not necessary. The intermittency can simply be set to unity within the

volume of propagation of the turbulent spot and the spot production rate can simply be set to zero in the volume of propagation of the spot and its becalmed region. Since the measurements of Seifert have been taken in the plane of symmetry of the turbulent spot, the results can effectively be treated as if they were obtained from a fully turbulent strip that has been triggered at the same stream-wise position. The velocities of the leading and trailing edge of the turbulent spot are taken as  $0.88U_\infty$  and  $0.5U_\infty$  respectively. These are well accepted zero pressure gradient values that are also confirmed in Seifert's experiment. The velocity of the rear of the becalmed region was set to the generally quoted value of  $0.3U_\infty$ .

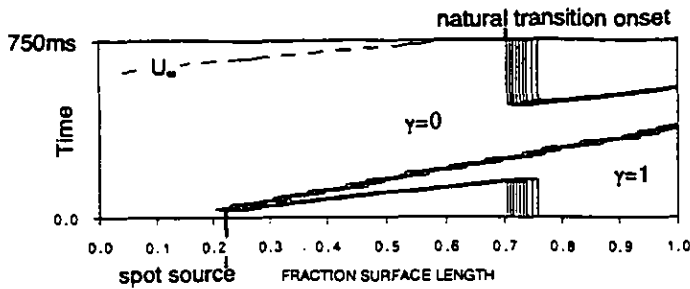


Figure 4: Simulated unsteady intermittency distribution of Seifert's test case (individual spot triggered at 20% $s$ )

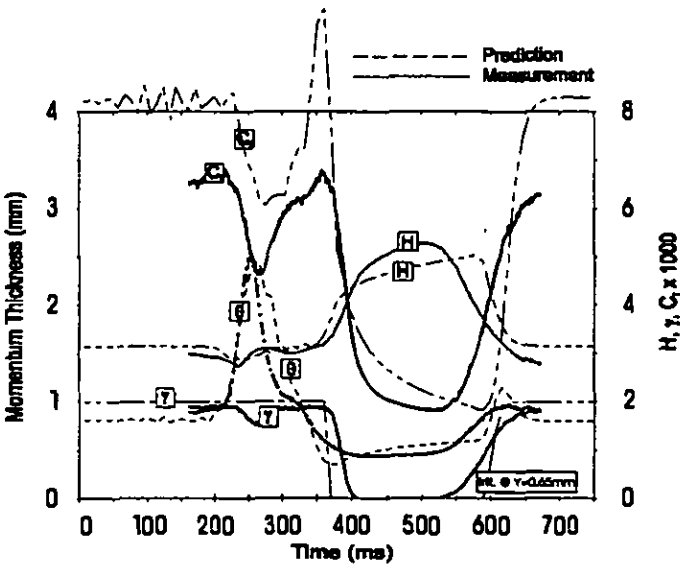


Figure 5a: Measured and predicted variation in time of integral boundary layer parameters at trailing edge for Seifert's test case

Figure 5a shows the variation in time of the integral boundary layer parameters at the trailing edge for the measurements and the predictions. Selected measured and predicted instantaneous (ensemble averaged in the case of the measurements) velocity profiles are shown in fig. 5b. At this position (trailing edge) the undisturbed boundary layer is fully turbulent, so the intermittency is unity. The

intermittency is shown in fig. 5a. It is not possible to identify the leading edge of the turbulent spot, since the intermittency is unity before the spot arrives, but it is possible to identify the trailing edge of the spot. After the spot has passed the intermittency drops to zero for the duration of the becalmed region. This happens approximately between  $t=370ms$  and  $t=600ms$  for the measurements and the predictions. In the case of the measurements the jump from unity to zero and the jump from zero to unity is not as sharp as for the predictions. However, the fact that the measurements show zero intermittency for approximately the same time interval as the predictions is important. It shows that the basis of the presented model concerning the effect of the becalmed region on the transition process, namely that no spots form inside the becalmed region, but that spots can move into it, appears fundamentally correct.

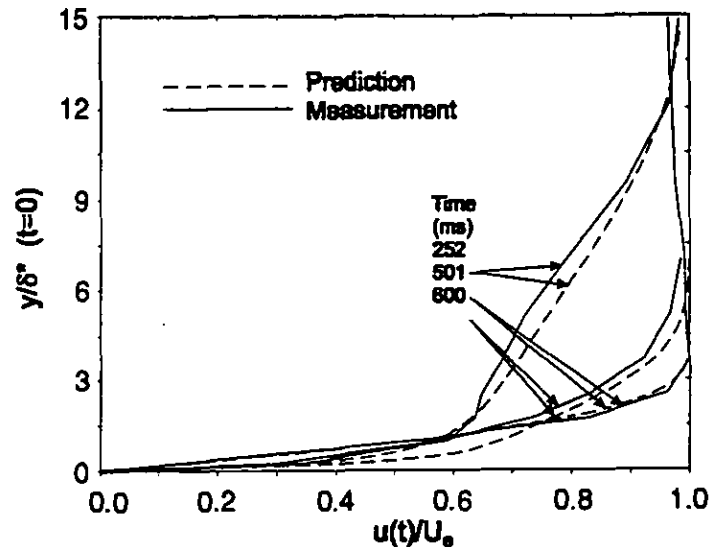


Figure 5b: Measured and predicted instantaneous velocity profiles at the trailing edge for Seifert's test case

There is a second aspect of the becalmed region which has, as mentioned above, not been explicitly modelled in the intermittency model. This is the specific velocity profile of the becalmed region and its possible ability to suppress laminar separation. Whereas the effect of the becalmed region on the transition process, which has been modelled, can be seen from the intermittency factor, the specific velocity profiles of the becalmed region can be inferred from the integral boundary layer parameters in fig. 5a and are also shown in fig. 5b.

The comparison of measurements and predictions in fig. 5a and fig. 5b reveals that more than just the main features of the integral boundary layer parameters and the velocity profiles could be predicted. This in particular refers to the region of the becalmed region between  $t=370ms$  and  $t=600ms$ , where the intermittency factor is zero and therefore the turbulence model is not active. The becalmed region is merely an unsteady response of the boundary layer to the almost instant vanishing of the turbulent stresses after a turbulent region has passed. Therefore the becalmed region is predictable by simulating the rapid vanishing of the turbulent stresses. It is concluded, that the becalmed region is modelled by the unsteady

laminar boundary layer equations and is therefore predictable by any unsteady boundary layer or Navier-Stokes solver independent of any turbulence modelling. Its effect on the transition process however needs to be either modelled in conjunction with an eddy viscosity model and the present intermittency model or can perhaps be predicted by higher order turbulence models which have some inherent capability of predicting transition. The other main effect of the becalmed region, the suppression or delay of laminar separation, is automatically accounted for by the unsteady boundary layer or Navier-Stokes equations and can be predicted (see below).

The details of the flow shown in fig. 5a are discussed using the example of the skin friction coefficient. The small differences in the absolute magnitude of the skin friction are very likely to be caused by the difficulties in extracting the skin friction coefficient from the hot-wire measurements. The changes in skin friction and the qualitative character of the curve are well predicted. After the arrival of the turbulent spot the skin friction coefficient starts to drop at approximately  $t=230\text{ms}$ . It arrives at a local minimum at about  $t=270\text{ms}$ , which is a short period after the displacement and the momentum thickness had their peak values (approximately  $t=250\text{ms}$ ). The lower skin friction in the spot affected region is due to the turbulent boundary layer inside the spot having grown for a longer time than the surrounding undisturbed turbulent boundary layer. Therefore the high momentum and displacement thickness, which are also caused by the 'long grown' turbulent boundary layer inside the turbulent spot almost coincide with a minimum in skin friction (see also Cumpsty et al., 1995).

As the turbulent spot leaves the measurement station, the skin friction rises to a peak at  $t=370\text{ms}$ . This is where the intermittency drops from unity to zero and where the momentum and displacement thickness have their minima. This peak in skin friction at the trailing edge of the turbulent spot and the beginning of the becalmed region is caused by the overshooting velocity close to the wall. This is because once the turbulent stresses disappear the low velocity in the outer part of the boundary layer rapidly increases towards the laminar value (in the becalmed region). This also affects the fluid in the inner part of the boundary layer which is also accelerated by shear forces and causes the high velocity gradient in the inner boundary layer region. This in turn causes the minima in displacement and momentum thickness which relate to a very transient very steep velocity gradient close to the wall at this instant in time. After the overshoot in the near wall region, the velocity close to the wall reduces at a much slower rate towards the value of an undisturbed laminar boundary layer. The velocity profile closely follows the form  $U^+=Y^+$ , as noted by Cumpsty et al. (1995), for the period of the becalmed region. After the peak the skin friction rapidly reduces to a very low value that it possesses throughout the becalmed region from approximately  $t=400\text{ms}$  to  $t=600\text{ms}$ . The minimum is reached at the end of the becalmed region at approximately  $t=600\text{ms}$ . When the intermittency rises from zero to unity at the end of the becalmed region the skin friction rises to the undisturbed turbulent value.

## ENTROPY GENERATION IN THE BECALMED REGION

### Calculation of the Dissipation in the Becalmed Region

The previous section presented measurements and predictions of the variation in time of the integral boundary layer parameters and the skin friction coefficient for Seifert's test case. The low value of skin friction and the low momentum thickness within the becalmed region that were noted above suggest that the entropy generation within this region is low.

From the conservation of entropy it can be shown (Denton, 1990) that the rate of entropy production per unit surface area is given by

$$\dot{S} = \frac{1}{T_0} \int_0^{\delta} \mu_t \left( \frac{\partial u}{\partial y} \right)^2 dy. \quad (2)$$

The non-dimensional dissipation coefficient is then defined by

$$C_d = \frac{T\dot{S}}{\rho U_{\infty}^3} \quad (3)$$

The dissipation coefficient has been evaluated for Seifert's test case. The prediction performed in order to evaluate the dissipation coefficient differs in one point from the prediction in the previous section that simulated the experiment. The undisturbed boundary layer has been taken as fully turbulent from 70%, so that the intermittency factor is always zero or unity. This simplification was introduced so that the effect of 'turbulent wetted area' could be assessed.

Figure 6 shows a distance-time diagram of the dissipation coefficient for this calculation. The leading edge area is signified by high entropy production. This is expected from the laminar boundary layer theory because the Reynolds-number is very low at the leading edge. The origin of the turbulent spot is located at approximately 17% and  $t=25\text{ms}$ . The area enclosed by the leading edge and the trailing edge trajectory of the spot exhibits a dissipation coefficients that is predominantly between 0.0015 and 0.0018. The undisturbed fully turbulent boundary layer downstream of 72% has dissipation coefficients that range from 0.0015 to 0.0021. The most important observation however is that the dissipation coefficient in the becalmed region is on the same low level as that of the normal laminar boundary layer at the same Reynolds-number. The values range between 0.0003 and 0.0006. The becalmed region only generates as much entropy as a laminar boundary layer, but it is not as susceptible to transition or separation.

### The 'Wetted Area' Assumption

A striking feature of fig. 6 is that downstream of 20%, the dissipation coefficient of the laminar boundary layer and the becalmed region is almost constant (around 0.0005) and independent of surface position. The same applies for the dissipation coefficient in the turbulent boundary layer of the undisturbed boundary layer and inside the spot affected area. The value ranges around 0.0018. This is in line with the general observation that in a Reynolds-number range where laminar or turbulent boundary layers can exist (momentum thickness Reynolds-number between 200 and 700), the dissipation coefficient of either state is only very weakly dependent on the momentum thickness Reynolds-number (Truckenbrodt, 1973).

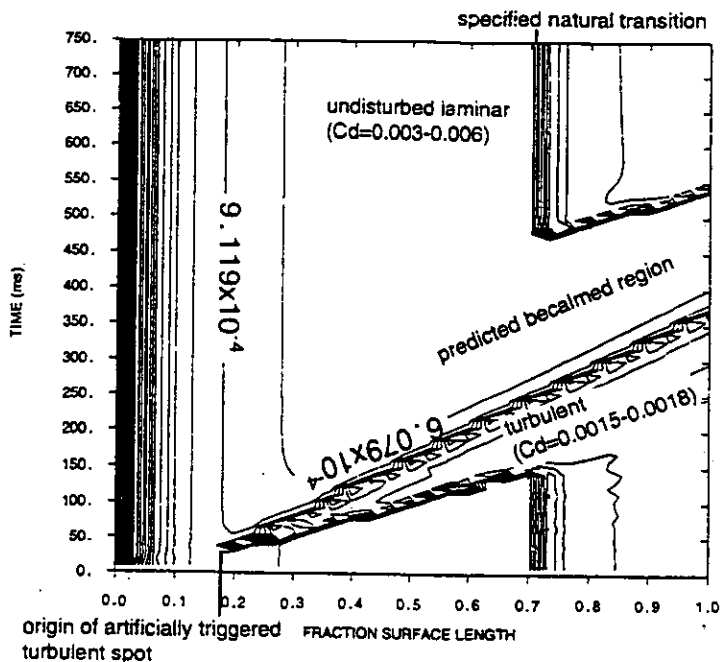


Figure 6: Contours in the distance-time diagram of dissipation coefficient for an individual turbulent spot triggered at 17%*s* and a (undisturbed) fully turbulent boundary layer from 70%*s*

The above observations allow us to postulate that any increase in loss is directly proportional to the additional 'turbulent wetted area' caused by the wakes. This hypothesis leads to a simplified quantitative assessment of losses generated in unsteady boundary layers. It presumes that any unit of surface covered by turbulent flow generates the same amount of entropy regardless of surface position and time. Furthermore, it is assumed that any unit of surface covered by laminar or becalmed flow generates the same amount of entropy regardless of surface distance and time. The wetted area assumption allows to draw conclusions about, for example, the relative increase in loss in a wake-induced unsteady boundary layer in relation to the loss generated by a completely laminar boundary layer simply by relating the ratios of the areas in the distance-time space that are covered by turbulent respectively laminar flows. Hodson (1989) used a similar approach to derive a correlation that relates the blade profile loss to the reduced frequency of the wake passing for attached boundary layers. That correlation did not account for the effect of the becalmed region because the data it was validated against did not suggest that this was important.

Schulte (1995) showed that for attached boundary layers no significant loss reduction due to the effect of the becalmed regions is possible. This is because the additional loss generated by, for example, a wake-induced turbulent patch in an otherwise laminar boundary layer will always almost compensate for the loss reduction due to the associated becalmed region in an otherwise turbulent boundary layer. This can also be seen from fig. 6, if one now imagines that the turbulent region (fully turbulent spanwise band) is the result of a narrow passing wake rather than an individual turbulent spot. As a function of wake-passing frequency, the loss will be almost constant at low frequency and then rise linearly with frequency once the

succeeding wake-induced turbulent patches start to cut off the preceding becalmed regions.

## SEPARATED BOUNDARY LAYERS AND HIGH LIFT LP TURBINE BLADING

Up to now, the prediction of the unsteady transition process in separated boundary layers with the above presented method is not possible. This is because not enough is known about the interaction of the becalmed region with the transition process in a separation bubble. Turbulent spots are not necessarily involved in separation bubble transition and hence the extension of Emmons spot-based model (see appendix) might not adequately describe the process.

Schulte and Hodson (1996) showed that for a high lift LP turbine cascade blade, the becalmed regions, which were caused by simulated wake-passing significantly reduced the loss compared to a no-wake case. This is because the suction surface boundary layer of the high lift blade separates if there are no wakes present. Figure 7 is taken from Schulte and Hodson. It was observed that in a separated boundary layer the becalmed region was not terminated by intruding spots from separated flow transition (supporting the above suspicion), so enhancing the effect of the becalmed region. Also, the loss associated with the separation can be very high at low Reynolds-numbers, so that the gain due to the becalmed region, which keeps the boundary layer attached is larger than the loss due to the additional turbulent flow upstream of the separation.

Schulte and Hodson (1996) also found that an optimum wake-passing frequency exists. The optimum frequency corresponds to the situation sketched in the distance-time diagram of fig. 7. Figure 7 represents a first crude model of the interaction of the becalmed region with the transition process in the separation region. This will certainly have to be refined in the future. One may assume that no grossly (and 'lossy') separated flow exists for this situation. Though the flow cannot be predicted using the presented intermittency routine, the loss may at least be estimated from the 'wetted area' assumption.

In fig. 7 one can treat the becalmed region as laminar (as suggested by fig. 6) as well as the small separated area (which is assumed to be justified, since the separation bubble will take some time to gain the shape it would adopt if no wakes were present, see Schulte, 1995). The region marked 'transitional' will be assumed to be fully turbulent. The reduced frequency will be assumed to be fixed at the optimum value which corresponds to the situation of fig. 7 (this is representative for LP turbines). Then the area ratios in fig. 7 yield the relation

$$\frac{Y_p - Y_{p,lam}}{Y_{p,turb} - Y_{p,lam}} = \frac{A_{turb}}{A_{ABCD}} \quad (4)$$

for the suction surface boundary loss coefficient. Assuming the well accepted zero pressure gradient values of  $1.0U_\infty$  for the leading edge propagation speed of a turbulent patch,  $0.5U_\infty$  for the trailing edge and  $0.33U_\infty$  for the rear of the becalmed region the boundary layer loss coefficient approximates to

$$Y_p \equiv Y_{p,lam} + 0.25(Y_{p,turb} - Y_{p,lam}) \quad (5)$$

where  $\gamma_{p,turb}$  is the loss generated by a fully turbulent boundary layer from the onset of wake-induced transition and  $\gamma_{p,lam}$  is the loss of a completely laminar boundary layer.

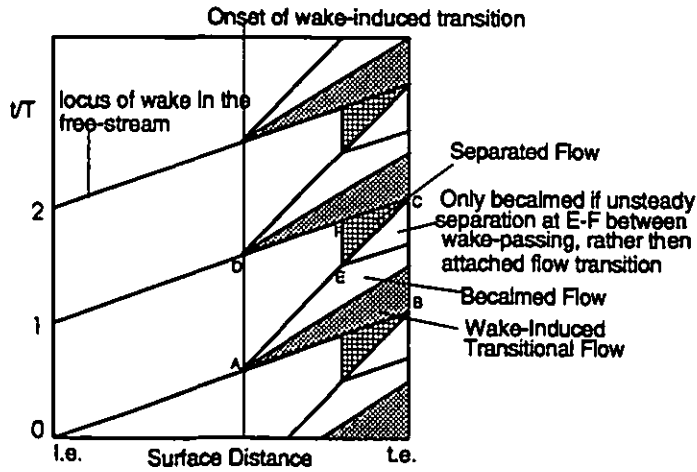


Figure 7: Schematic distance-time diagram showing effect of becalmed region on a separated boundary layer and illustrating optimum wake-passing frequency

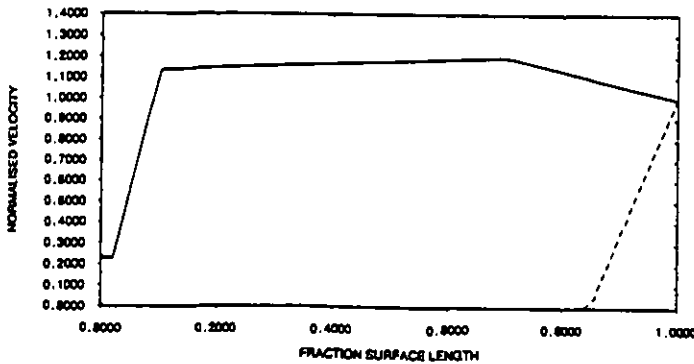


Figure 8: Example of generic velocity distribution used for parametric design study

Equation (4) can now be used to perform a parametric design study. For this purpose generic velocity distributions of the type shown in fig. 8 are produced. They feature different back surface diffusion and Zweifel-lift coefficients. Wake-induced transition (fully turbulent) is assumed to take place at  $Re_{th}=200$ . This is before the start of laminar separation in all cases. In order to evaluate the boundary layer loss coefficient, the values for  $\gamma_{p,turb}$  and  $\gamma_{p,lam}$  must be found.

The value of  $\gamma_{p,turb}$  can simply be found by performing a steady boundary layer calculation and specifying transition where  $Re_{th}=200$ . This will give a value for the momentum thickness at the trailing edge, which represents the loss generated in the boundary layer. This can be converted into a loss coefficient by dividing by the pitch (which is proportional to the Zweifel-lift coefficient in incompressible flow).

The value of  $\gamma_{p,lam}$  can be found by performing an unsteady calculation with the present boundary layer code by specifying an intermittency distribution of the type shown in fig. 4. This merely serves the purpose to generate some laminar (becalmed flow) at the trailing edge in order to extract a laminar value of the momentum thickness at the trailing edge. This is possible if the simulated becalmed region suppresses the laminar separation that would otherwise be predicted by the code. The momentum thickness at the trailing edge at the rear of the becalmed region (where it has almost relaxed to the undisturbed value) will be taken as an indicator of the loss that would be generated if the boundary layer were completely laminar (or becalmed). This momentum thickness will be converted into a loss coefficient in the same way as the turbulent momentum thickness.

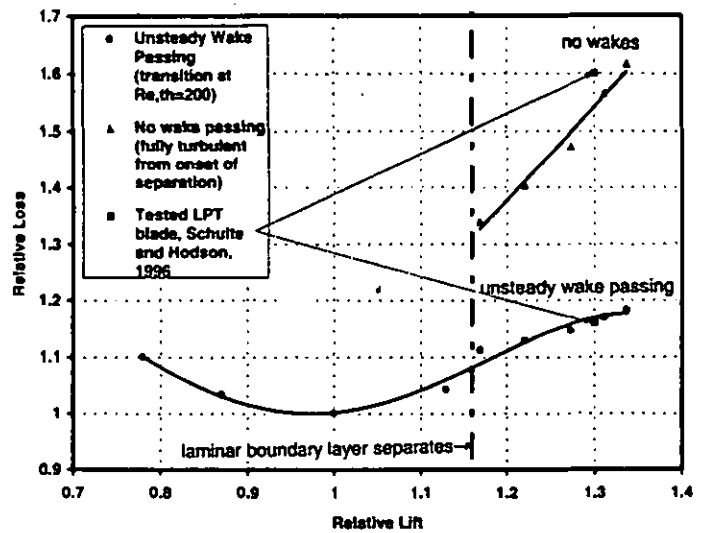


Figure 9: Numerical design study using model of fig. 7 and wetted area assumption showing suction surface loss only ( $Re_2=1.3 \times 10^5$ ,  $Re_{th}=200$ )

The results of the study are presented in fig. 9. The study has been performed at  $Re_2=130000$  (which is representative of a low Reynolds-number LPT environment). The results of the study are the points labelled as 'unsteady wake-passing'. There is an optimum lift coefficient calculated, which is of the order of traditional optimum Zweifel-lift coefficients. For the five cases with the highest lift coefficients the boundary layer code predicts laminar separation, if no transition or unsteady wake passing is specified. If an unsteady calculation is performed with the unsteady intermittency distribution as an input, then the code predicts the boundary layer to stay attached inside the becalmed region. This confirms the earlier statement that the ability of the becalmed region to suppress separation is predictable. At even higher lift and diffusion coefficients (not shown here), the becalmed region separated.

The most important observation from fig. 9 is that at relative lift values above 1.16 (where laminar separation occurs if there is no transition, thick dotted line) the unsteady wake passing cases show a significantly reduced rise in loss compared to the relative loss evaluated from a simulation without unsteady wake passing (assuming

a fully turbulent boundary layer from onset of laminar separation). The difference in absolute level of the two loss curves is not claimed to be accurate, since in reality the no-wake case features a separated rather than a fully turbulent boundary layer. At this low Reynolds-numbers the loss for the separated boundary layer in the no-wake case is likely to be even higher as the calculated fully turbulent loss. This is indicated by the measured data from the high lift LP turbine blade from Schulte and Hodson, 1996, where the data point with wake passing has been fitted to the calculations in order to compare the relative increase of the loss if there is no wake passing.

The results show that high lift blading, owing to the becalmed regions, has more potential than for example a steady state cascade test or numerical study would suggest. A 15% increase in lift (from 1.16 to 1.34) only results in 7% increase in boundary layer loss when wake passing effects are present, while it results in approximately 21% increase in boundary loss from steady state considerations.

The real benefit of high lift blading is of course application specific and must take the reduction of blade numbers (weight and manufacturing cost) into account. This should for many aircraft engine applications lead to the result that a slight increase of profile loss is perfectly acceptable (Curtis et al. (1996)). In order to estimate the magnitude of increased profile loss, studies of the type presented in this paper accounting for the effect of the becalmed region may be performed.

## CONCLUSIONS

1) The becalmed region which trails wake-induced turbulent patches inside boundary layers is an unsteady boundary layer feature which is modelled by the laminar unsteady boundary layer equations. It is therefore predictable independent of any turbulence modelling.

2) The effect of the becalmed region on the transition process can be modelled using a probability-based intermittency approach, similar to the Emmons model.

3) The entropy generation inside the becalmed region is on the same level as in a conventional laminar boundary layer

4) The becalmed region is less prone to separation than a conventional laminar boundary layer.

5) The loss of an attached boundary layer cannot be significantly reduced due to unsteady wake passing, despite the beneficial effect of the becalmed region.

6) Design criteria for high lift blading may be derived from the 'wetted area assumption'. The loss of higher lift blading subjected to unsteady wake-passing does not rise to the same extent as for steady fully turbulent or separated boundary layers.

## ACKNOWLEDGEMENTS

During his time at the Whittle Laboratory the first author was in receipt of grants from the Engineering and Physical Sciences Research Council of the UK, the Cambridge University Engineering Department and the Flughafen Frankfurt Main Stiftung.

## REFERENCES

- Addison, JS, and Hodson, HP, 1992, "Modelling of Unsteady Transitional Boundary Layers", ASME Jnl. of Turbomachinery, Vol. 114, No. 3, pp 580-589, Jul.
- Banieghbal, MR, Curtis, EM, Denton, JD, Hodson, HP, Huntsman, I, Schulte, V, Harvey, NW, Steele, AB, 1995, "Wake Passing in LP Turbine Blades", presented at the AGARD conference, Derby, UK, 8.5.-12.5. 1995
- Cebeci, T, and Carr, LW, 1978, "A Computer Program for Calculating Laminar and Turbulent Boundary Layers for Two Dimensional Time Dependent Flows"; NASA TM 78470, March 1978,
- Cumpsty, NA, Dong, Y, LI, YS, 1995, "Compressor blade boundary layers in the presence of wakes", presented at the IGTI conference in Houston, Texas, 1995
- Curtis, EM, Hodson, HP, Banieghbal, MR, Denton, JD, Howell, RJ, 1996, "Development of blade profiles for low pressure turbine applications", ASME-paper 96-GT-???, 1996
- Denton, JD, 1990, "Entropy generation in turbomachinery flows", 7th Cliff Garrett Turbomachinery Award Lecture, SAE paper 902011
- Emmons, HW, 1951, "The laminar-turbulent transition in a boundary layer- Part 1", Journal of Aerospace Science, Vol. 18, No7, pp490-498
- Gostelow, JP, Walker, GJ, Solomon, WJ, Hong, G, Melwani, N, 1996, "Investigation of the calmed region behind a turbulent spot", ASME-paper 96-GT-489
- Halstead, DE, Wisler, DC, Okiishi, TH, Walker, GJ, Hodson, HP, Shin, H, 1995, "Boundary layer development in axial compressors and turbines" Part 1-4, presented at the IGTI conference in Houston, Texas
- Hodson, HP, 1984, "Boundary Layer and Loss Measurements on the Rotor of an Axial Flow Turbine", ASME Jnl. of Engineering for Gas Turbines and Power, Vol. 106, April
- Hodson, HP, 1989, "Modelling Unsteady Transition and Its Effects on Profile Loss", Proceedings, AGARD conf. PEP 74a on Unsteady Flows in Turbomachines, AGARD CP 468. Also ASME Jnl. of Turbomachinery, Vol. 112, No 4, Oct. 1990, pp 691-701
- Hodson, HP, Huntsman, I, Steele, AB, 1994, "An investigation of boundary layer development in a multistage LP turbine", ASME Jnl. of Turbomachinery, Vol 116, July, pp 375-383
- Hourmouziadis, J, 1989, "Aerodynamic Design of Low Pressure Turbines", AGARD Lecture Series, 167
- Narasimha, R, 1957, "On the Distribution of Intermittency in the Transition Region of a Boundary Layer", Journal of Aerospace Science, Vol. 24, pp 711-712.
- Pfeil, H, Herbst, R, and Schröder, Th, 1982, "Investigation of Laminar-Turbulent transition of boundary layers disturbed by wakes", ASME paper 82-GT-124
- Seifert, A, 1994, "The turbulent spot as a stabilising agent of a transitional boundary layer", submitted for publication in the 'Journal of Fluid Mechanics'
- Schubauer, GB, and Klebanoff, PS, 1955, "Contributions on the Mechanics of Boundary Layer Transition", NACA TN 3489 (1955) and NACA Rep. 1289 (1956)
- Schulte, V, 1995, "Unsteady Separated Boundary Layers in Axial-flow Turbomachinery", PhD Dissertation, Cambridge University



Schulte, V, Hodson, HP, 1996, "Unsteady wake-induced boundary layer transition in high lift LP turbines", ASME-paper 96-GT-486, 1996

Truckenbrodt, E, 1973, "Neuere Erkenntnisse über die Berechnung von Strömungsgrenzschichten mittels einfacher Quadraturformeln", Part I Ing. Arch. 43, 9-25 (1973), Part II Ing. Arch. 43 136-144 (1974)

## APPENDIX

Consider the  $(x,z,t)$ -space as sketched in fig. A1. The  $x$  and  $z$  co-ordinates are the stream-wise and span-wise co-ordinates of a boundary layer and  $t$  is the time co-ordinate. The figure shows by analogy with a figure from Emmons (1951) a section of the dependence volume of a turbulent spot  $V_{dep1}(x,z,t)$  and in addition that of a turbulent spot and its becalmed region  $V_{dep2}(x,z,t)$ . The dependence volume  $V_{dep1}(x,z,t)$  comprises all those points in the  $(x,z,t)$ -space that could have been the origin of a turbulent spot that made the point  $P(x,z,t)$  turbulent. Its shape is determined by the stream-wise and span-wise growth rates of turbulent spots. The dependence volume  $V_{dep2}(x,z,t)$  contains all those points in the  $(x,z,t)$ -space that could have been the origin of a turbulent spot that made the point  $P(x,z,t)$  turbulent or becalmed. Its shape is determined by the stream-wise and span-wise growth rates of turbulent spots and becalmed regions. The intersection with the  $xz$ -plane shows the plan view of a turbulent spot (simplified triangular shape ABC) and its becalmed region (BDEC).

The probability, that the flow at a given point  $P(x,z,t)$  in the  $(x,z,t)$ -space is turbulent was given by Emmons (1951) by the expression

$$\gamma(x,z,t) = 1 - \exp\left[-\iiint_{V_{dep1}(x,z,t)} g(x_0, z_0, t_0) dx_0 dz_0 dt_0\right]. \quad (A1)$$

Here  $g(x,z,t)$  denotes the spot production rate, which is a function of space and time. The spot production rate at any given point  $P_0(x_0, z_0, t_0)$  is defined as the number of spots formed in an infinitesimal volume  $dV_0 = dx_0 dz_0 dt_0$  at point  $P_0(x_0, z_0, t_0)$ .

The expression (A1) is derived for the  $(x,z,t)$ -space. It is generally valid for steady and unsteady flows. In order to be able to calculate the intermittency (probability)  $\gamma(x,z,t)$  one needs to specify the spot production function  $g(x,z,t)$  and one needs the geometry of the volume of dependence, which is governed by the spreading angles and the propagation rates of a turbulent spot. It was concluded above that spot production is inhibited by a becalmed region following a turbulent spot, as it is underneath the turbulent spot itself. This was sketched in fig. 2.

Following the above argument, the formation of a turbulent spot and a becalmed region at point  $P_0(x_0, z_0, t_0)$  inside the enlarged volume of dependence  $V_{dep2}(x,z,t)$  (as sketched in fig. A1) renders the spot production function  $g(x,z,t)$  at point  $P(x,z,t)$  equal to zero. Not all spots formed in the enlarged volume of dependence will pass through  $P(x,z,t)$  but if the spots do not their becalmed regions will. Consequently, the spot production function inside the enlarged volume of dependence  $V_{dep2}(x,z,t)$  has an effect on the spot production function  $g(x,z,t)$  at point  $P(x,z,t)$ . Therefore, the spot production rate  $g(x,z,t)$  has an effect on the spot production at downstream locations. To take proper account of the effect of

becalmed regions, one needs an expression to correct the distribution of the spot production rate  $g(x,z,t)$  which can then be used in Emmons expression (A1) to calculate the intermittency.

The desired expression can be derived by using the same principle as that used to derive equation (A1). The probability, that point  $P(x,z,t)$  in fig. A1 is turbulent or becalmed is by analogy with equation (A1) given by

$$p_{tc}(x,z,t) = 1 - \exp\left[-\iiint_{V_{dep2}(x,z,t)} g_{cor}(x_0, z_0, t_0) dx_0 dz_0 dt_0\right] \quad (A2)$$

The corrected spot production function  $g_{cor}(x_0, z_0, t_0)$  within the volume of dependence  $V_{dep2}(x,z,t)$  is assumed to be known at this stage of the analysis. The probability  $p_{tc}(x,z,t)$  also corresponds to the probability that the spot production function  $g(x,z,t)$  at point  $P(x,z,t)$  is zero. The initially specified probability that a spot forms at  $P(x,z,t)$  is given by  $g(x,z,t) dx dz dt$ . The corrected probability that a spot forms at  $P(x,z,t)$  is the initial probability times the probability that  $P(x,z,t)$  is neither turbulent nor becalmed. This yields

$$g_{cor}(x,z,t) dx dz dt = g(x,z,t) dx dz dt \cdot (1 - p_{tc}(x,z,t)) \quad (A3)$$

Substituting equation (A2) into equation (A3) one obtains

$$g_{cor}(x,z,t) = g(x,z,t) \cdot \exp\left[-\iiint_{V_{dep2}(x,z,t)} g_{cor}(x_0, z_0, t_0) dx_0 dz_0 dt_0\right] \quad (A4)$$

for the corrected spot production rate at point  $P(x,z,t)$ . After the entire distribution of the corrected spot production rate  $g_{cor}(x,z,t)$  has been found, it can then be used in equation (A1) instead of  $g(x,z,t)$  to calculate the distribution of the intermittency. The calculation can proceed by marching downstream from a starting position where the spot production rate is negligible.

In practice, the omission of the correction of the spot production function (equation A4) does not have any relevance for steady flow transition, because Narasimha's concentrated breakdown hypothesis states that the spot production rate is zero downstream of the breakdown position.

The presented extension of Emmons theory to calculate the intermittency has to be applied if one wants to take account of the becalmed regions in unsteady flow transition.

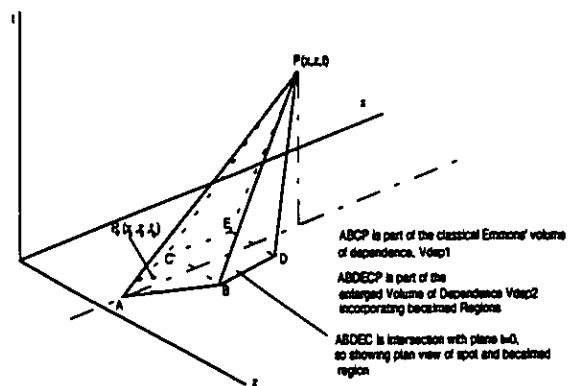


Figure A1: Schematic of dependence volumes of a turbulent spot and its becalmed region